Appl. Phys. A (2016) 122:513
DOI 10.1007/s00339-016-0039-2

Applied Physics A
Materials Science & Processing

Mixed proton and electron conduction in graphene oxide films: field effect in a transistor based on graphene oxide

V. A. Smirnov[1] · A. D. Mokrushin[2] · V. P. Vasiliev[1] · N. N. Denisov[1] · K. N. Denisova[3]

Received: 19 February 2016 / Accepted: 1 April 2016 / Published online: 13 April 2016

Abstract GO films exhibited dual proton and electron conduction. Proton conduction showed the exponential dependence on relative humidity with the activation energy $E_a = 0.9 \pm 0.05$ eV. For the electron conductivity (220–273 K) induced by thermolysis and chemical means $E_a = 1.15 \pm 0.05$ eV. With increasing humidity, the electron conduction went down, which was associated with recombination phenomena. The GO films can be regarded as a first example of the mixed electron–proton conduction when sample conductivity can be regulated by external influence (humidity). Field effect is detected and studied in the transistor on the basis of the GO in different types of conduction.

1 Introduction

Attention to graphene and related materials sharply increased after isolation of graphene nanosheets in 2004 [1]. Initially, graphene oxide (GO) was regarded just as a starting material for preparation of graphene, but nowadays GO is suggested as a candidate for use in a variety of materials and devices, which are devoted to reviews [2–7]. The process of obtaining the GO, methods of reducing and use of materials on the basis of reduced the GO are considered in the above reviews. The electrical properties of the GO films also investigated in a number of works. In the papers [8–10], the proton conductivity of multilayer films of GO was studied and it was noted [9–11] that photoreduction of GO leads to the onset of electronic conductivity accompanied by concomitant decay of protonic conductivity. Materials with mixed conductivity type are used in various devices, as discussed in the review articles [12–14]. Electron–ion conductivity in inorganic materials [12] and electron–proton in conducting polymers [13, 14] are generally regarded as the total conductivity in these materials. A recent trend is the development of composite materials comprising of two components exhibiting the protonic and electronic conductivity. In such composites, the role of matrix is usually played by nafion while that of electron-conducting component, by reduced graphene oxide [15], carbon nanotubes [16], and metal hydrides [17]. In these materials electron conductor is actually a foreign body in the nafion matrix so that the electronic conductivity of the material depends on the quality of contact between the constituents. In wet conditions the protonic conductivity can be expected to grow, while the electronic one to decrease due to insulation of particles with electronic conductivity. In contrast to composites, GO is a homogeneous material but in OG films exhibiting protonic conductivity in wet conditions [9–11] it seems feasible to induce electronic conductivity under the action of external influences, such as thermal treatment, chemical processing, and UV irradiation.

Field effect (FE) in transistors with a thin 2D carbon canal up to the graphene monolayer deposited on the surface of single-crystalline plate oxidized silicon was implemented and studied in detail in the fundamental work

✉ N. N. Denisov
ndenisov@cat.icp.ac.ru

[1] Institute of Problems of Chemical Physics, Russian Academy of Sciences, Academician Semenov Avenue 1, Chernogolovka, Moscow Region, Russia 142432

[2] Institute of Microelectronics Technology and High Purity Materials, Russian Academy of Sciences, Academician Osip'yan St. 6, Chernogolovka, Moscow Region, Russia 142432

[3] Faculty of Physics, Lomonosov Moscow State University, GSP-1, Leninskie Gory, Moscow, Russia 119991

K.S. Novoselov et al. [1]. The paper was also studied magnetic phenomena in these transistors. This work caused the explosive interest in objects such as graphene, and results of researches can be found in review articles [18–20]. Researches of FE transistors based on graphene and oxidized silicon performed in [21–23]. The article [21] reports about field effect on the reduced graphene oxide monolayer, and this effect is several percent. In [22], the mobility of charge carriers was investigated in a wide temperature range. In [23], a shift of the Dirac point for graphene surface treatment by electron beam of 30 keV is observed. In [24], in FE transistors the modified graphene (heterostructure) is used, allowing to change the current 4–5 orders of magnitude by gate voltage. In [25], using the graphene oxide as an insulating layer is proposed. The use of graphene oxide in the FE transistor considered in [26]: The conductive layer graphene is created on the layer of GO by hydrogen plasma, and GO served as an insulating layer on the gate. Graphene oxide was also used as an insulating layer in a transistor deposited on a flexible plastic, wherein the active layer and electrodes graphene are used [27]. It should be noted that GO in a humid atmosphere of the insulator becomes a conductor with proton conductivity, while the reduction of the GO leads to the appearance of electronic conductivity [8]. The influence of such properties on the GO characteristics of electronic devices has not been studied in the literature. The task of this paper is: (a) to investigate the behavior of the conductivity of multilayer GO films with the joint of the electron and proton conductivity in the same sample and (b) to examine the influence of the cross-electric field on the electron–hole and the proton conductivity of the GO film deposited on SiO_2/Si plate type of field effect transistor.

2 Experimental

Synthesis of GO and preparation of its aqueous suspension were carried out as described elsewhere [8, 9]. A measuring device with interdigitated Cu contacts was made by casting aqueous suspension of GO of a required concentration on a fiberglass substrate. An interelectrode distance was 0.3 mm. Experiments were carried out mostly with GO films 100 ± 20 nm thick, as confirmed by interference pattern. Electric measurements were taken by using a P-30S potentiostat. Two-probe method was used to conduct measurements, which is consistent with the measurements in the field effect transistor.

Chemical reduction of GO was carried out in hydrazine hydrate vapor at a 25–60 °C [5]; thermal reduction was performed at 130 °C. Relative humidity (RH) was set by using tabulated pressures of water vapor over saturated solutions of various salts. The circuit of transistor for research field effects is shown below, and the film thickness in the GO therein was about 1 μm measured by profiler Talystep firm Taylor-Hobson, UK.

3 Results and discussion

3.1 Protonic conductivity

The GO films deposited on the electrodes and dried at room temperature reveal conductivity in wet conditions [8, 9], and the GO films that cast onto a substrate are known to exhibit the electroconductivity of typical proton conductors [8–10, 28]. Figure 1 shows typical behavior of current i through a GO film upon variation in relative humidity (RH). The insert shows the σ(RH) function plotted in semilogarithmic coordinates.

Changes in protonic current i upon stepwise variation in applied voltage U ($\Delta U = 50$ mV, RH 53 %) are presented in Fig. 2. It follows that current i is proportional to applied voltage U.

The temperature dependence of protonic conductivity σ was found (Fig. 3) to be linearized (for $T > 0$ °C) in the Arrhenius coordinates with the activation energy $E_a = 0.9 \pm 0.05$ eV. The latter is close to that (0.83 eV) reported for the membranes made of GO paper [29]. The close value of $E_a = 0.78 \pm 0.03$ eV was found for proton transport through a one-atom-thick graphene layer [30].

3.2 Electron conductivity

After partial reduction of GO, our films exhibited also electron conduction. Cells with GO film are dried and reduced in several ways: chemically and thermally: In all cases the electronic component of current is occurred in the dry samples. Figure 4 shows the i–U characteristics of GO

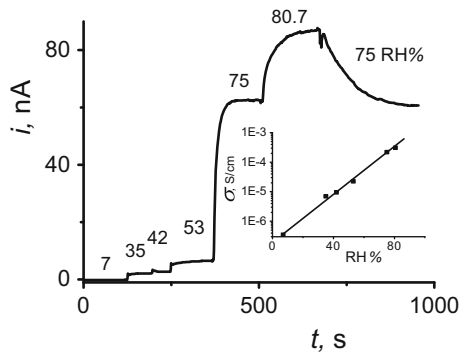

Fig. 1 Behavior of current i through a GO film upon variation in relative humidity (RH); $U = 0.5$ V. The insert shows the σ(RH) function plotted in semilogarithmic coordinates

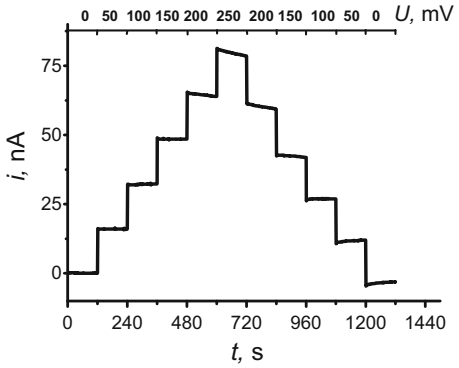

Fig. 2 Changes in protonic current i upon stepwise variation in applied voltage U: $\Delta U = 50$ mV; RH 53 %

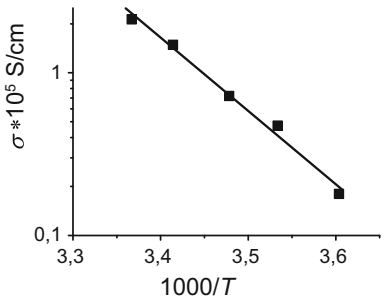

Fig. 3 Temperature dependence of protonic conductivity σ as plotted in the Arrhenius coordinates (RH 75 %, $U = 0.3$ V)

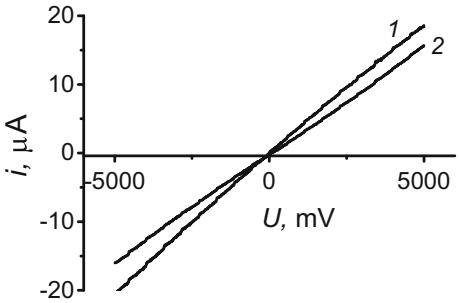

Fig. 4 The i–U characteristics of GO films (RH 7 %) after partial reduction of GO: *1* by annealing at 130 °C for 3 h, and *2* in hydrazine vapor (25–60 °C, 50–75 h, $U = \pm 5$ B, RH 7 %)

films (at RH 7 %) after partial reduction of GO: (1) by thermal treatment at 130 °C for 3–4 h and (2) by chemical means in the pair of hydrazine at 50–75 h at a temperature of 25–60 °C (treatment conditions were adjusted to get comparable current characteristics).

The linearity of i–U characteristics did not depend on the duration of each reduction procedure. At the initial stages of reduction (when contribution from electron conduction is low), some nonlinearity may be introduced by proton conduction depending on the ambient humidity. The

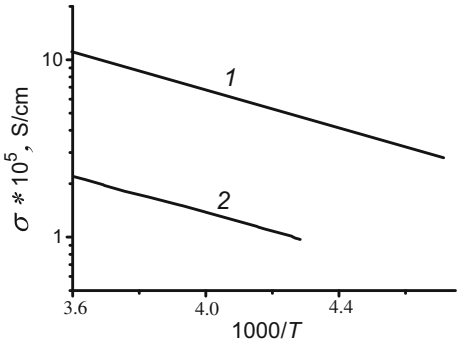

Fig. 5 Electron conductivity σ versus $1000/T$ ($T < 0$ °C) for GO films after their *1* treatment with hydrazine vapor and *2* annealing at 130 °C for 3 h

linearity of our i–U characteristics agrees with the results [31] reported for structurally defected multilayer graphene films (300 nm thick) after their oxidation with oxygen plasma, and the conductivity of the layer has changed (decreased) in the oxidation process but the current–voltage characteristics remained linear.

The temperature dependence of electronic conductivity σ was found (Fig. 5) to be linearized (for $T < 0$ °C) in the Arrhenius coordinates, irrespective of the type of reduction method, and under these conditions, the water is frozen and there is no proton conductivity. For chemical (plot *1*) and thermal (plot *2*) reduction the activation energies were estimated as $E_a = 1.15 \pm 0.05$ eV in both cases. In the temperature range 220–273 K, our conductivity results well fit the exponential dependence $\sigma \sim \sigma_0 \exp(-\Delta E/kT)$. This implies that the conductivity is governed by a single barrier, which is the case for typical semiconductors. In amorphous materials, such as conductive polymers conductivity described by hopping model [32], in this case, the temperature in the exponent must have a power relationship of the type $T^{1/n}$, where n ranges from 1 to 3. But this dependence is manifested at low temperatures, which is not investigated in our case.

3.3 Overall conductivity

Partially reduced GO films exhibited both electron and proton conduction: In ambient condition RH 7 % it is electronic conductivity, while in wet conditions (RH 35 %), it is protonic one (Fig. 6). Applying voltage U to partially reduced GO at RH 7 % gives rise to electron current i(e) (see Fig. 6). Upon sample insertion into wet conditions (RH 35 %), current i is seen to sharply decrease.

At the first glance it looks strange since, according to Fig. 1, this must be accompanied by the onset of proton conduction. In contrast to inorganic crystals with mixed electron–hole conduction where the above currents are

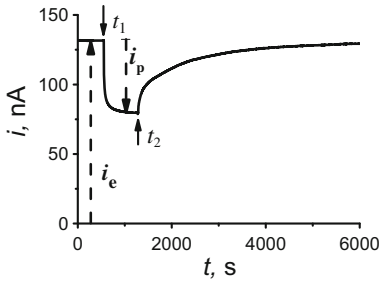

Fig. 6 Behavior of current i through a GO film partially reduced in hydrazine vapor. Time moments t_1 and t_2 indicate sample insertion into wet (RH 35 %) and ambient (RH 7 %) conditions, respectively

summarized, in our case they are deducted. A main process responsible for a drop of overall current in Fig. 6 can be the electron trapping by positively charged oxonium ions followed by their recombination with protons. Sample return to ambient humidity (moment t_2 in Fig. 6) restores the electron current up to its initial level.

Figure 7 illustrates the behavior of current i through a GO film upon variation in RH after chemical reduction to different starting values of i(e) As is shown in Fig. 7a, after the first stage of reduction (to i(e) = 107 nA) an increase in RH initially decreases current i and then causes its growth: This implies that the protonic conductivity becomes larger than the electronic one. Upon further reduction to i(e) = 140 nA (Fig. 7b), the overall view of the i(RH) function markedly changes because the electron conductivity becomes larger than the protonic one even at high RH 75 %. The GO is converted in graphene material after a long reduction, current in the film is due to the electronic component only, and it is independent of humidity essentially.

It should be noted that the electronic component is not fully compensated by the protonic one. This means that the channels for electron conduction appear in the GO film after any kind of treatment due to sp^2 hybridization, and such channels cannot be closed by moisture diffusing along the surface of layers with sp^3 hybridization with hydroxy and epoxy groups. Tentatively, this can be said about proton conduction: After each kind of processing, the GO film still retains some channels with sp^3 hybridization due to the presence of hydroxy and epoxy groups suitable for diffusion of water molecules and hence for proton conduction. Such channels do not overlap. But in some film areas the domains of electron and proton conductivities may nevertheless overlap.

Since in wet conditions GO films behave as typical proton conductors [8–10, 28], the effect of mixed conduction can be exhibited by other materials with simultaneous electron and proton conductivity. Similar decrease in electron conduction with increasing humidity observed for

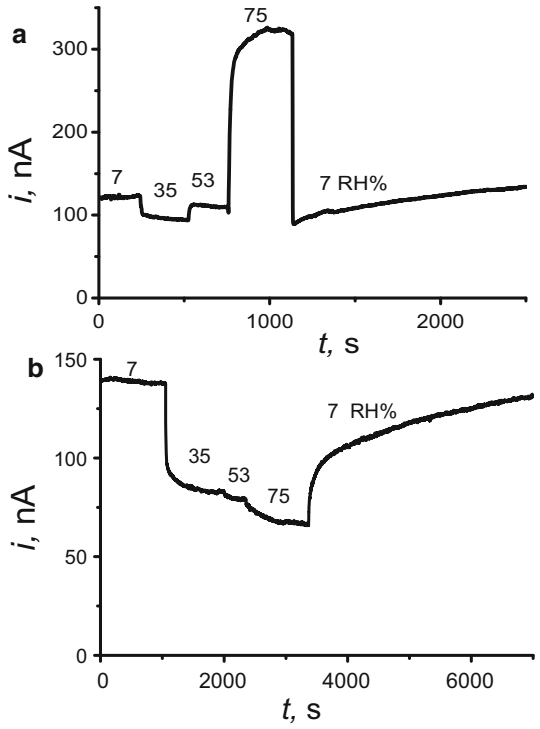

Fig. 7 The dependence of the total current from the humidity in the GO film after the reduction in hydrazine vapor: **a** partial reduction in hydrazine vapor to i(e) = 107 nA and **b** additional reduction to i(e) = 140 nA

composite materials [15–17] was associated with insulation of electron-conducting particulates upon moisturizing. It is possible that in these cases a recombination channel reduces electron conductivity when moist. In our case, the observed decrease in the overall conductivity cannot also be explained by screening the domains electron conduction since the OG film is not a composite material, comprising of uniform GO sheets.

3.4 Relaxation processes

The difference between the properties of the electron and the proton conductivity affects relaxation processes. Figure 8 shows the transient current characteristics of a step change of voltage on the sample. Curve 1 corresponds to the change of the electron current in a partially reduced film of GO when applying a voltage +1 and −1 to the electrodes in 1-min intervals. It can be seen the curves of changes in the current square, which is typical for the inertialess current component in the sample. The protonic constituent comparable with electronic conductivity appears when placing the same sample in a humid atmosphere of 53 % RH (curve 2). The transient characteristics manifested relaxation component of the current. Further increase in humidity to 75 % RH (curve 3) significantly

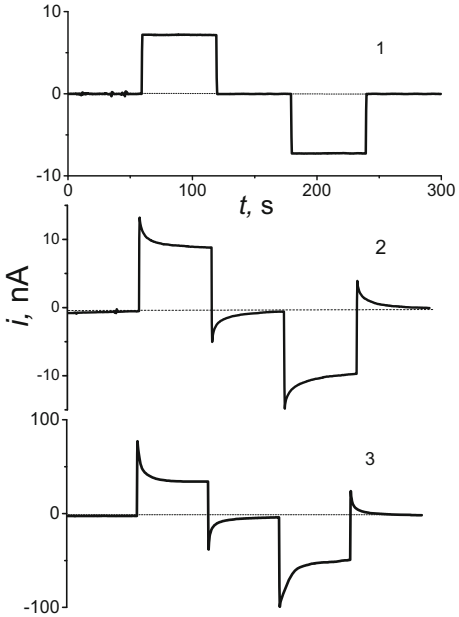

Fig. 8 Transient current characteristics at a step change in the voltage of +1 and −1 V, the interval of 60 s. *1* Electronic conductivity of the GO film RH 7 %; *2* total conductivity at 53 % RH; *3* total conductivity at 75 % RH

increased the current, and the proton relaxation component becomes comparable to stationary current.

Relaxation (Fig. 8) is not described by a monoexponential dependence, and the relaxation time (at half height) is several seconds. Dipole polarization of water molecules and charged fragments with the attached water may be responsible for such processes. Relaxation is due not only to the electronic component, but also to the structural, that is their rotating and partial displacement. Such fragments may be, e.g., H_2O_2 groups, arising during attachment of water molecules to the hydroxy group, and the proton of the group participates in conduction. Our transient characteristics are consistent with the frequency dependency of the impedance measured for GO films at various humidities [33]: The amplitude of impedance decreases with increasing the frequency and with increasing the environments humidity.

3.5 Model of field effect transistor

The presence of two types of conduction in the GO films can be shown by using the GO in the circuit of field effect transistor. Field effect was studied both in a proton and an electron–hole conduction of GO in the transistor circuit shown in Fig. 9. The GO film thickness was about 1 μm, the thickness of the SiO_2 is 0.1 μm, the voltage $U_{sd} = 1$ V, and the gate (G) was applied step voltage from 0 to ±12 V in 1.5 V.

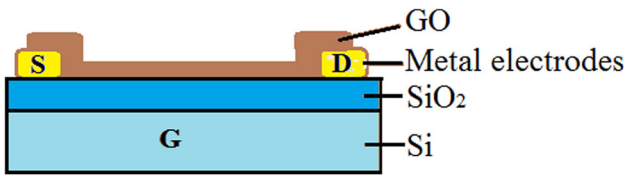

Fig. 9 The circuit of transistor

Figure 10 shows the current characteristics of the proton conductivity of the transistor—only unreduced GO is present in the sample wherein cannot be the electronic conductivity. There is no current ($i < 1$ nA) even when applied to the gate voltage U_g of −12 to 12 V in a dry atmosphere at the source–drain voltage $U_{sd} = 1$ V. At placing transistor in a humid atmosphere RH 75 % (time t_1) the current appears in a sample due to proton conductivity (Fig. 1). The current reaches saturation after about a minute, and then, voltage negative step is applied to the gate. The supply negative voltage substantially increases the current. At a positive voltage to the gate this current of the transistor begins to decrease (after 300 s) and even changes sign when the $U_g = 6$ V. Current reduction can be attributed to the electron–proton recombination. As can be seen from Fig. 10, every time you switch the gate voltage, relaxation phenomena occur—current peaks with a gradual decline to a steady-state current value.

The subsequent partial reduction of GO leads to the appearance of electron–hole conductivity (Fig. 11). The initial current $i_0 \approx 120$ nA, and the current depends on the degree of reduction of the GO. Field effect in this case significantly changes the amplitude of response—when applying a positive voltage to the gate the increase in transistor current (right peak in Fig. 11a) is observed, which corresponds to the electronic conductivity in the layer of the GO. These currents are three orders of magnitude superior to proton conduction currents. It is seen that the current hole (left peak in Fig. 11a) is about twice weaker electron and this can be explained by differences in the values of the drift mobility of electrons and holes.

Figure 12 shows the linear anamorphosis plots shown in Figs. 10 and 11. It should be noted qualitative and quantitative field effect difference between the proton and electron–hole conductivity. First, there is a change in the direction of current upon variation in the sign of voltage applied to the gate: a negative voltage enhances the current of the proton conductivity and a positive voltage increases the electronic conductivity. Secondly, current greatly increases at the electronic conductivity at the same gate voltages compared with proton conductivity—this effect can be explained by the different mobility of charges (electrons, holes, and protons) in different cases.

From Fig. 12a it is seen that proton conduction currents at positive offsets remain virtually unchanged and are not

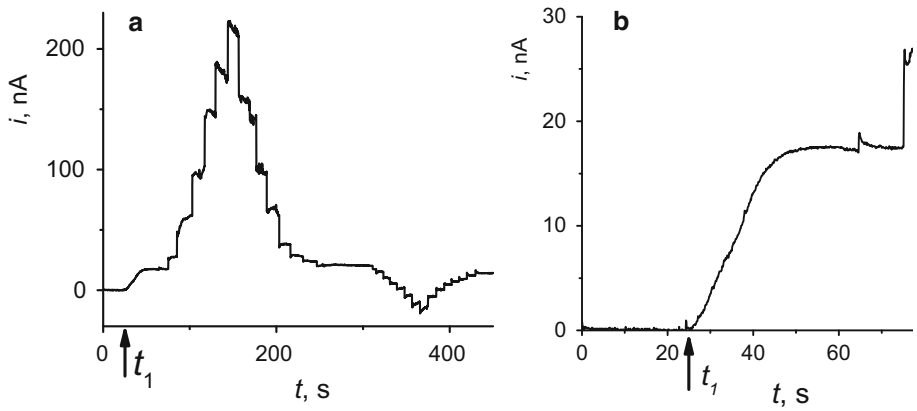

Fig. 10 The proton conductivity. **a** Current transistor characteristics when placed in a humid atmosphere 75 % RH, and the gate voltage is changed stepwise in the range 0–(−12 V) to 0–(+12 V) to 0 step 1.5 V, $U_{DS} = 1$ V. **b** The initial section of Fig. 10a

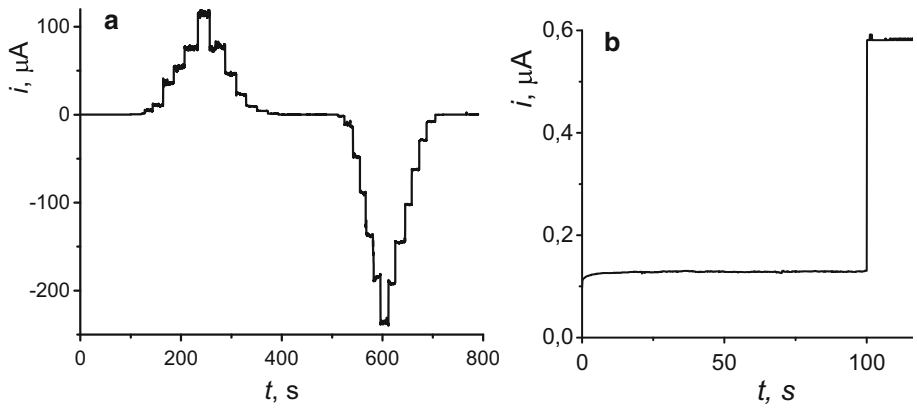

Fig. 11 The electron–hole conductivity. **a** The current characteristics of transistor in the dry sample (RH < 7 %) after partial reduction of the GO film by hydrazines vapor, electron conduction current i(e) ~ 120 nA. Measurement conditions are the same as in Fig. 10. **b** The initial section of Fig. 11a

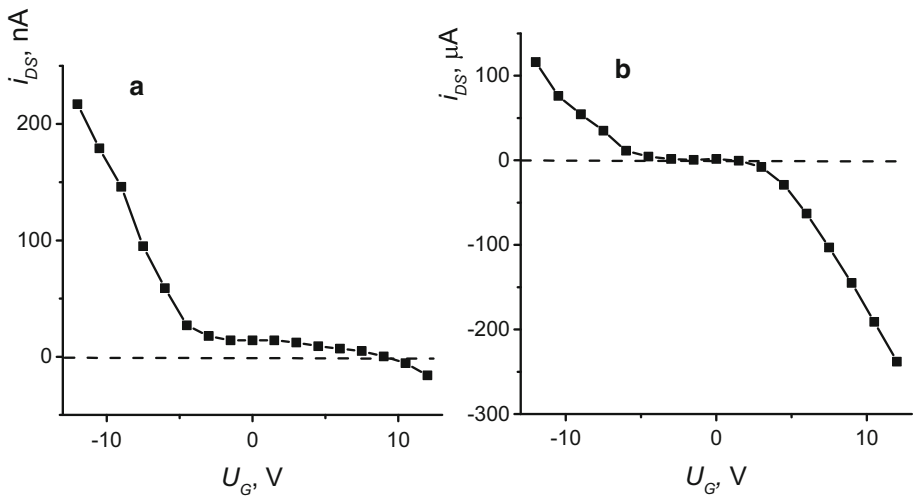

Fig. 12 **a** The dependence of the current on the transverse electric field at proton (built from the data in Fig. 10) and **b** electron–hole conductivity of the transistor (built from the data in Fig. 11)

of interest. The left branch of this figure (negative bias) allowed us to estimate the concentration of proton conductivity at various displacements. In this case the value of the drift mobility of the protons is taken to be the value obtained in [34] for ice at a temperature of −5 °C: $\mu_p = 6.4 \times 10^{-3}$ cm^2/Vs. The concentration of protons at zero bias $n_p = 0.4 \times 10^{17}$ cm^{-3}, and $U_g = -12$ V $n_p = 4.4 \times 10^{17}$ cm^{-3}, that is, the proton concentration at that offset, is increased an order of magnitude. Analysis of Fig. 12b at electron–hole allows to obtain values of the conductivity of the drift mobility of electrons and holes at different U_g, based on the total ratio $\sigma = ne\mu$ and considering that $U_{sd} = 1$ V. For example, when a bias voltage $U_g = 10$ V, the electron mobility ($\mu_e = 1.2 \times 10^2$ cm^2/

Vs), and hole mobility ($\mu_h = 0.6 \times 10^2$ cm^2/Vs), which is approximately two times lower than the electronic one. It should be noted that in [35] the ratio of electron to hole mobility is reverse that observed by us for the graphene layer, the hole mobility ($\mu \approx 10^4$ cm^2/Vs) being significantly higher than our values. This is quite natural, since the graphene film has a much more perfect structure than thick (tens or even hundreds of times) films of the GO, in which graphene sheets are arranged randomly, and their recovery is made partially.

Our data are consistent with results of other authors on the measurement of the field effect in materials with proton conductivity: polysaccharides [36] and Nafion [37]. Significant field effect in a humid atmosphere is observed in these materials; for example, polysaccharides proton conductivity is shown at humidity RH > 50 % [36].

4 Conclusions

GO films can exhibit dual proton and electron conduction. Proton conduction shows the exponential dependence on relative humidity and temperature with the activation energy $E_a = 0.9 \pm 0.05$ eV at the temperature range T > 0 °C. For the electron conductivity (220–273 K) induced by thermolysis and chemical means $E_a = 1.15 \pm 0.05$ eV. With increasing humidity, the electron conduction goes down, which can be associated with recombination phenomena. The GO films can be regarded as a first example of the mixed electron–proton conduction when sample conductivity can be regulated by external influence (humidity). Such properties may play a significant role in the devices based on graphene oxide, e.g., a field effect transistor. The field effect transistor based on the GO at a certain degree of reduction can demonstrate as a proton and an electron–hole conductivity. In the latter case, the currents of the transistor are approximately three orders of magnitude larger than the currents of proton conductivity. These phenomena can be used to control the properties of the transistor, for example, in sensor circuitry and transducers. On the other hand, ambient humidity can substantially affect the operations stability of the field effect transistor with the GO as an insulating layer.

Acknowledgments This research work was supported by the Russian Foundation for Basic Research (Project No. 16-29-06263).

References

1. K.S. Novoselov, A.K. Geim, S.V. Morozov, D. Jiang, Y. Zhang, S.V. Dubonos, I.V. Grigorieva, A.A. Firsov, Science **306**, 666 (2004)
2. Y. Zhu, S. Murali, W. Cai, X. Li, J.W. Suk, J.R. Potts, R.S. Ruoff, Adv. Mater. **22**, 3906 (2010)
3. O.C. Compton, S.B.T. Nguyen, Small **6**, 711 (2010)
4. M.J. Allen, V.C. Tung, R.B. Kaner, Chem. Rev. **110**, 132 (2010)
5. V. Singh, D. Joung, L. Zhai, S. Das, S.I. Khondaker, S. Seal, Prog. Mater. Sci. **56**, 1178 (2011)
6. Y.-L. Zhang, L. Guo, H. Xia, Q.-D. Chen, J. Feng, H.B. Sun, Adv. Opt. Mater. **2**, 10 (2014)
7. F. Perrozzi, S. Prezioso, L. Ottaviano, J. Phys.: Condensed Matter **27**, 013002 (2015)
8. V.A. Smirnov, N.N. Denisov, A.E. Ukshe, Y.M. Shulga, Chem. Phys. Lett. **583**, 155 (2013)
9. N.N. Denisov, V.A. Smirnov, Y.M. Shulga, *Chapter 4. Graphene Oxide Films: Photochemistry and Electroconductivity*, in *Graphene Oxide (Synthesis Mechanical Properties and Applications)*, ed. by Ryana Boveri (NOVA Science Publishers Inc, New York, 2014), pp. 93–161
10. M.R. Karim, K. Hatakeyama, T. Matsui, H. Takehira, T. Taniguchi, M. Koinuma, Y. Matsumoto, T. Akutagawa, T. Nakamura, S.-I. Noro, T. Yamada, H. Kitagawa, S. Hayami, J. Am. Chem. Soc. **135**, 8097 (2013)
11. K. Hatakeyama, H. Tateishi, T. Taniguchi, M. Koinuma, T. Kida, S. Hayami, H. Yokoi, Y. Matsumoto, Chem. Mater. **26**, 5598 (2014)
12. I. Riess, Solid State Ion. **157**, 1 (2003)
13. G. Inzelt, M. Pineri, J.W. Schultze, M.A. Vorotyntsev, Electrochim. Acta **45**, 2403 (2000)
14. N. Costantini, G. Wegner, M. Mierzwa, T. Pakula, Macromol. Chem. Phys. **206**, 1345 (2005)
15. B.A. Aragaw, W.-N. Su, J. Ricka, B.-J. Hwang, RSC Adv. **3**, 23212 (2013)
16. M. Tortello, S. Bianco, V. Ijeri, P.S. Spinelli, E. Tresso, J. Membr. Sci. **415–416**, 346357 (2012)
17. A. Oberoi, J. Andrews, Int. J. Smart Grid Clean Energy **3**, 270 (2014)
18. M. Lemme, Solid State Phenom. **156**, 499 (2010)
19. F. Schwierz, Nat Nanotechnol. **5**, 486 (2010)
20. A.H. Castro Neto, F. Guinea, N.M.R. Peres, K.S. Novoselov, A.K. Geim, Rev. Mod. Phys. **81**, 109 (2009)
21. Z. Luo, Y. Lu, L.A. Somers, A.T.C. Johnson, J. Am. Chem. Soc. **131**, 898 (2009)
22. J.-H. Chen, C. Jang, S. Xiao, M. Ishigami, M.S. Fuhrer, Nat Nanotechnol. **3**, 206 (2008)
23. I. Childres, L.A. Jauregui, M. Foxe, J. Tian, R. Jalilian, I. Jovanovic, Y.P. Chen, Appl. Phys. Lett. **97**, 173109 (2010)
24. I.V. Antonova, I.A. Kotin, N.A. Nebogatikova, V. Ya, Prinz. Tech. Phys. Lett. **41**, 950 (2015)
25. G. Eda, A. Nathan, P. Wöbkenberg, F. Colleaux, K. Ghaffarzadeh, T.D. Anthopoulos, M. Chhowalla, Appl. Phys. Lett. **102**, 133108 (2013)
26. B. Standley, A. Mendez, E. Schmidgall, M. Bockrath, Nano Lett. **12**, 1165 (2012)
27. S.-K. Lee, H.Y. Jang, S. Jang, E. Choi, B.H. Hong, J. Lee, S. Park, J.-H. Ahn, Nano Lett. **12**, 3472 (2012)
28. V.A. Smirnov, N.N. Denisov, N.N. Dremova, Y.M. Vol'fkovich, A.Y. Rychagov, V.E. Sosenkin, K.G. Belay, G.L. Gutsev, N.Y. Shulga, Y.M. Shulga, Appl. Phys. A **117**, 1859 (2014)
29. R. Kumar, M. Mamlouk, K. Scott, Int. J. Electrochem. Article ID 434186 (2011)
30. S. Hu, M. Lozada-Hidalgo, F.C. Wang, A. Mishchenko, F. Schedin, R.R. Nair, E.W. Hill, D.W. Boukhvalov, M.I. Katsnelson, R.A.W. Dryfe, I.V. Grigorieva, H.A. Wu, A.K. Geim, Nature **516**, 227 (2014)
31. K. Kim, H.J. Park, B.-C. Woo, K.J. Kim, G.T. Kim, W.S. Yun, Nano Lett. **8**, 3092 (2008)

32. N.F. Mott, E.A. Davis, *Electron Processes in Non-Crystalline Materials*, 2nd edn. (Clarendon Press, Oxford, 1979)
33. Y. Yao, X. Chen, J. Zhu, B. Zeng, Z. Wu, X. Li, Nanoscale Res. Lett. **7**, 363 (2012)
34. M. Kunst, J.M. Warman, Nature **288**, 465 (1980)
35. B. Fallahazad, K. Lee, G. Lian, S. Kim, C.M. Corbet, D.A. Ferrer, L. Colombo, E. Tutuc, Appl. Phys. Lett. **100**, 093112 (2012)
36. C. Zhong, Y. Deng, A.F. Roudsari, A. Kapetanovic, M.P. Anantram, M. Rolandi, Nature Communications, 2:476, January 2011. doi:10.1038/ncomms1489, ISSN 2041-1723
37. K.L. Riskey, *Fabrication and Characterization of a Solid-State Ambipolar Ionic Field-Effect Transistor*. A Thesis for the Degree of Master of Science, 2013. http://dspace.library.colostate.edu/webclient/deliverymanager/digitool_items/csm01_storage/2013/06/15/file_1/207313